

# Transport properties of chitosan and whey blended with poly( $\epsilon$ -caprolactone) assessed by standard permeability measurements and microcalorimetry

I. Olabarrieta<sup>a,b</sup>, D. Forsström<sup>a,c</sup>, U.W. Gedde<sup>a</sup>, M.S. Hedenqvist<sup>a,\*</sup>

<sup>a</sup>Department of Polymer Technology, Royal Institute of Technology, SE-100 44 Stockholm, Sweden

<sup>b</sup>The Foundation Packforsk — The Swedish Packaging Research Institute, P.O. Box 9, SE-164 93 Kista, Sweden

<sup>c</sup>Thermometric AB, Spjutvägen 5A, SE-175 61 Järfälla, Sweden

Received 29 March 2000; received in revised form 12 July 2000; accepted 13 September 2000

## Abstract

Blends of poly( $\epsilon$ -caprolactone) (PCL) with chitosan and a whey-protein-isolate (WPI) were prepared by solution mixing and film casting. The purpose was to increase the water vapour resistivity of chitosan and whey by blending them with a hydrophobic biodegradable polymer. The water vapour transmission rate was determined by a standard technique and by a new technique based on microcalorimetry. The blends were characterised by scanning electron microscopy (SEM), density measurements and thermogravimetry. Oxygen permeability was measured on the pure components and on some of the blends. The incorporation of PCL yielded a pronounced decrease in water vapour transmission rate of both chitosan and the WPI measured at a relative humidity gradient of 11 to 0%. A volume content of 17–18% of PCL lowered the water vapour transmission rate by 70–90%. It was found that the majority of the PCL particles were ellipsoidal in chitosan and fibrous in the WPI and the data indicated that the particle shape had an important influence on the water vapour transmission rate. The large decrease in water vapour transmission rate was also due to a reduction in water solubility because of limited swelling of the constrained chitosan or WPI matrix in the presence of PCL. SEM revealed that the miscibility/compatibility between PCL and the matrices was good. The water vapour transmission rate of the films decreased with increasing vacuum-drying time of the chitosan and WPI solutions. Microcalorimetry provided accurate estimates of water vapour transmission rate. Furthermore, this technique proved to be very flexible and the water vapour transmission rate could be determined over a broad range of relative humidities in a single experiment. © 2001 Elsevier Science Ltd. All rights reserved.

*Keywords:* Chitosan; Whey; Transport properties

## 1. Introduction

Concern for the preservation of our biosphere has never been stronger than it is today. There is a great problem of disposal of plastics, because of their very low weight-to-volume ratio and their inalterability over very long durations of time. Today, incineration is a common method to get rid of polyolefines, but this unfortunately leads to high emissions of CO<sub>2</sub>. An interesting possibility is to use edible and biodegradable materials instead of non-renewable polymers, e.g. in packagings [1–3]. These materials have the potential to reduce environmental pollution by lowering solid disposal waste and reducing the need for incineration [4]. It has been shown that whey or whey-protein-isolates (WPI) and chitosan have good film-forming properties and

therefore have a potential for being used as polymer films [4–7].

Liquid whey, a by-product of cheese manufacturing, is produced in large quantities and its annual production is continuously rising [8]. The main components of liquid whey are whey-proteins, lactose, fat and inorganic minerals. Usually the whey is purified and the whey-protein content increased, a procedure that is very costly. Purification with respect to the whey-protein is performed to enhance its film-forming properties. The whey-protein is brittle and a plasticiser has to be added to make it possible to handle the film. Although whey is used in several fields, e.g. as animal feed, a lot of whey is still wasted. Consequently there is a significant interest in finding new applications for whey or whey-protein, e.g. as edible and biodegradable films [9].

Chitosan is produced by deacetylation of the naturally occurring chitin. Similar in structure to cellulose, chitin is one of the most abundant of all polysaccharides found in the

\* Corresponding author. Tel.: +46-8-790-76-45; fax: +46-8-20-88-56.

E-mail address: mikaelhe@polymer.kth.se (M.S. Hedenqvist).

natural environment. The sea-food industry produces large amounts of chitin that originate from the external skeleton of many insects and crustaceans, e.g. crabs and prawns. As in the case of whey, lots of chitin is wasted.

Because of the large number of hydrogen bonds in proteins and polysaccharides, films of these materials are good barriers to permanent gases and hydrophobic substances. Some of these materials also have good mechanical properties [10]. Unfortunately, the hydrogen bonds in these renewable materials make them sensitive to water, which prohibits their use in packaging. There is therefore a need to increase their water resistivity without losing their biodegradability. An interesting option is to blend chitosan and whey with poly- $\epsilon$ -caprolactone (PCL). PCL is a petroleum-based biodegradable polymer and it is one of the most hydrophobic polyesters existing today [11]. The objective of this paper is to report attempts to find a procedure to blend PCL with chitosan and whey, which yields good film properties and a blend morphology that yields good barrier properties. The influence of the film-making method on the pure chitosan and whey materials is also studied. A new method based on microcalorimetry that makes a rapid determination of water vapour permeability possible is developed, and it is compared with a standard technique for monitoring water vapour transmission rates.

## 2. Experimental

### 2.1. Materials

A WPI, Lacprodan DI-9224, was supplied by MD Foods Ingredients (Denmark). Chitosan of molar mass  $\bar{M}_w = 400\,000\text{ g mol}^{-1}$  was provided by Fluka Biochemika, Sweden. Glycerol, chloroform (tri-chloro-methane stabilised with 1% ethanol) were purchased from Lab-Scan (Sweden). PCL, grade: TONE P-300 ( $\bar{M}_w = 10\,000\text{ g mol}^{-1}$  and  $\bar{M}_w/\bar{M}_n = 1.7$ ) was supplied as granules from Union Carbide, USA. Acetic acid (glacial 100%) was purchased from MERCK.

### 2.2. Sample preparation

#### 2.2.1. Chitosan films

Acetic acid was used to protonise the chitosan molecule,  $\text{NH}_2 \rightarrow \text{NH}_3^+$ , in order to make the polymer more soluble in water. The most efficient way of preparing a chitosan solution was by first dissolving chitosan 1% (w/w) in water during high-speed stirring and adding acetic acid (1%) to the solution while stirring it. Stirring was continued for approximately 30 min until all chitosan was dissolved. To ensure a homogeneous solution, it was mixed in a blender for 4 min. The solution was kept unstirred for 2 h before it was decanted into petri-dishes covered by Teflon<sup>®</sup>-coated aluminium (BYTAC<sup>®</sup> from Norton Performance Plastics Corp.). Approximately 20 g of solution was poured into

each petri-dish. Films were dried for 48 h at room temperature and 30% relative humidity.

#### 2.2.2. WPI films

An aqueous solution of 12% whey (w/w) and 6% (w/w) of glycerol was stirred for 15 min at room temperature. The solution was kept at 73°C for 20 min in order to denaturalise the protein. The solution was then decanted into petri-dishes covered by Teflon<sup>®</sup>-coated aluminium (20 g in each) and subsequently dried for 48 h at room temperature and 30% relative humidity.

#### 2.2.3. PCL/chitosan films

An aqueous solution containing 1% chitosan (w/w) and 1% acetic acid (w/w) and a chloroform solution containing 10% PCL (w/w) were each decanted into separate glass tubes. Both solutions were mixed with a magnetic stirrer for 20 min. The chitosan solution was then mixed in a blender for 4 min and the PCL solution was subsequently added to the chitosan solution and the new solution was mixed for another 4 min. The solution was left for 30 min and it was then dried in a vacuum oven for 10 min before it was decanted into petri-dishes covered by Teflon<sup>®</sup>-coated aluminium (20 g solution was decanted in each dish). Air, which was dissolved in the solution, was removed by vacuum-drying. Films were subsequently obtained after the solution had dried for 24 h at 23°C and 30% relative humidity. Blends were prepared with 5, 10 and 15% by weight of PCL with respect to the chitosan added.

#### 2.2.4. PCL/WPI films

The WPI and the PCL solutions were made as described above. The solutions were separately stirred until homogeneous solutions were obtained and they were then mixed together in a blender for 4 min. The new solution was cooled to room temperature. Subsequently a layer of foam was removed from the surface of the solution and the solution was then heated to 60°C for 20 min. After a second cooling to room temperature, the solution was allowed to dry in a vacuum oven for 10 min before it was decanted into petri-dishes covered by Teflon<sup>®</sup>-coated aluminium (25 g solution in each dish) at 23°C and 30% relative humidity. Blends were prepared with 5, 10 and 15% by weight of PCL with respect to the WPI added.

### 2.3. Methods

#### 2.3.1. Water vapour transmission rates

The water vapour transmission rates were measured using a Mocon Permatran-W Twin at 23°C according to ASTM F 1249-90. The water vapour transmission rate was normalised with respect to the polymer layer thickness. A pad with a saturated LiCl solution was placed at the bottom of the test cups to expose the films to 11% relative humidity during the permeability measurements. The upper side of the films was kept at 0% relative humidity. Prior to testing, the specimens

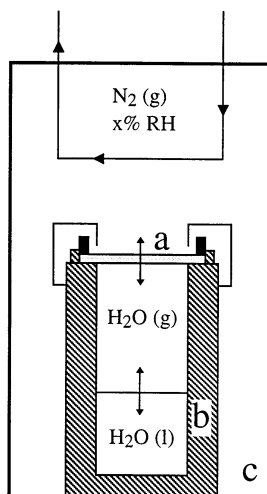


Fig. 1. Details of the 4-ml perfusion ampoule: (a) sample film, (b) stainless steel ampoule, and (c) perfusion ampoule.

were conditioned for 48 h in an environmental chamber at 23°C and 11% relative humidity on the high-pressure side and 0% relative humidity on the low-pressure side.

### 2.3.2. Microcalorimetry

A microcalorimeter system (2277 Thermal Activity Monitoring, Thermometric AB, Sweden) of the heat conduction type equipped with a 4-ml stainless steel RH perfusion ampoule (2255-010), referred to as TAM, was used for the measurements [12]. The RH perfusion ampoule was designed to humidify a gas to a specified relative humidity by mixing a flow of dry gas with a flow of gas of 100% relative humidity. A flow rate of 1 ml min<sup>-1</sup> was used by means of a mass flow controller. A closed and empty 4-ml stainless steel ampoule was used on the reference side. The calorimeter was calibrated using an internal calibration power of 300 μW. The baseline was adjusted by using gas flow over an empty perfusion ampoule. The experimental set-up is shown in Fig. 1. Nitrogen gas is flushed in the upper compartment of the perfusion ampoule. The film sample is tightly fastened onto the upper part of the steel ampoule by a stainless steel ring that is anchored using a screw. To ensure no leakage, vacuum-grease was applied between the film and the steel ampoule. In the present case, water was added to the lower compartment, i.e. inside the steel ampoule. The measurement principle is based on the assumption that there is an equilibrium exchange of water molecules between the liquid, the lower compartment, the film and the upper compartment at steady-state. It is also assumed that the heat of condensation at the lower film surface is the same as the heat of evaporation at the upper film surface and that the heat of solution and desolution of water in the film are included in these terms. The calorimetric response at steady-state measured by the microcalorimeter is the heat flow due to evaporation of water from the liquid. The water vapour transmission rate at

steady-state through the film,  $Q_o$ , is given by:

$$Q_o = \frac{P_e M t}{\Delta H_v A \Delta p} \quad (1)$$

where  $P_e$  is the heat flow rate,  $M$  is the molar mass of water and  $t$  is the film thickness.  $A$  is the exposed surface area of the film ( $A = 0.2827 \text{ cm}^2$ ) and  $\Delta p$  is the water vapour pressure difference across the film. The heat of water evaporation from the liquid ( $\Delta H_v$ ) was measured for pure water by first putting 0.4 g of water into a steel ampoule with an inner diameter of 6 mm, which in turn was inserted into the perfusion ampoule (Fig. 1). Before insertion, the water-containing steel ampoule was weighed. The perfusion ampoule was inserted into the TAM according to the general procedure recommended by the manufacturer. After approximately 60 min, the calorimetric response corresponded to the thermal activity of the specimen. A 3-ml-min<sup>-1</sup> nitrogen gas flow was used to dry the perfusion ampoule before calibration and after each measurement, and the flow of nitrogen in the upper compartment was kept at 1 ml min<sup>-1</sup> during the measurements. After approximately 15 h, the perfusion ampoule was withdrawn and the steel ampoule was weighed. The mass loss of water and the heat consumption during this period enabled the heat of evaporation of water to be calculated. The value obtained was 44.5 kJ mol<sup>-1</sup>, which is in agreement with reported data at 25°C [12]. An almost constant heat flow was monitored throughout the complete 15-h period, which indicates that steady-state conditions were rapidly attained. In order to achieve a relative humidity of 11% in the lower compartment, a solution saturated with LiCl crystals was used instead of pure water. The heat of evaporation of water in this case was obtained by a procedure similar to that for pure water. The endothermic heat flow decreased slightly during the 19 h of testing and an average heat flow was therefore used in the calculations. The value obtained for the heat of evaporation of water for the LiCl solution was 42.2 kJ mol<sup>-1</sup>. In a third method, the lower compartment was kept effectively at 0% relative humidity with dehydrite (anhydrous Mg(ClO<sub>4</sub>)<sub>2</sub>). In this case, a flow of water vapour from the upper to the lower compartment was obtained by letting humid nitrogen gas flow in the upper compartment. The relative humidity of the nitrogen gas was adjusted between 0 and 27.5%. It is, however, possible to obtain any relative humidity gradient through the polymer film by the use of the microcalorimeter technique.

### 2.3.3. Oxygen transmission rates

The permeability of the material to oxygen at 298.2 K was determined using a Mocon OX-TRAN TWIN equipped with a coulometric oxygen sensor. Degassed film samples with thickness of 60–300 μm were mounted in an isolated diffusion cell and were subsequently surrounded by flowing nitrogen gas to remove sorbed oxygen from the samples. The sample had a circular exposure area of  $5 \times 10^{-4} \text{ m}^2$  achieved by covering a part of the film with a tight

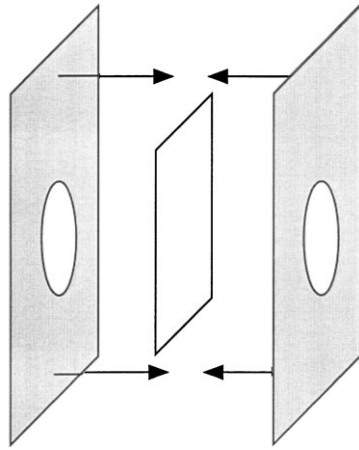


Fig. 2. A polymer sample glued together in between two aluminium foils with circular holes of  $5 \times 10^{-4} \text{ m}^2$ .

aluminium foil that has an adhesive on its surface (Fig. 2). One side of the sample was initially exposed to flowing oxygen containing 1% hydrogen at atmospheric pressure. The oxygen pressure was zero on the other side. The flow rate ( $Q$ ) through the sample was measured and, from the steady-state flow rate ( $Q_\infty$ ), the oxygen permeability coefficient ( $P$ ) was calculated.

#### 2.3.4. Density measurements

The densities of the samples at 296.2 K were determined by weighing in air and in *n*-hexane with a Mettler-Toledo AE 163-balance and applying the Archimedes principle.

#### 2.3.5. Scanning electron microscopy (SEM)

SEM was performed on fractured cross-sections of gold–palladium sputtered specimens using a JEOL JSM-5400 scanning electron microscope.

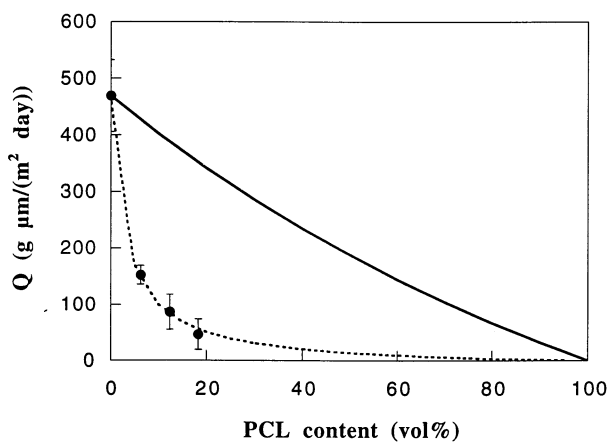


Fig. 3. Water vapour permeability ( $Q$ ) of PCL/chitosan (●). The solid line is from the Maxwell equation and the broken line is the fitted curve according to the Fricke model using an aspect ratio  $w/t = 150$  for the less permeable particles.

#### 2.3.6. Thermogravimetry

Thermogravimetry was performed by heating 10 mg samples at  $20^\circ\text{C}/\text{min}$  from  $25^\circ\text{C}$  to  $250^\circ\text{C}$  using a Mettler-Toledo TGA-SDTA 851 thermogravimeter.

### 3. Results and discussion

Fig. 3 shows the water vapour transmission rate for PCL/chitosan films as a function of PCL content. The improvement in water barrier properties with increasing PCL content was substantial. The blend containing 18.3 vol% (15 wt%) PCL exhibited a decrease in  $Q$  of 90%, compared with that of pure chitosan. Maxwell derived a relationship for predicting the electrical conductivity of a system of low-conducting spheres in a high-conducting matrix [13]. The assumption in this derivation is that the content of spheres is low enough to ensure that no direct contact exists between neighbouring spheres. Considering the physical similarity between solute permeability and electrical conductivity, it is possible to apply the Maxwell equation to the present system. Predicted data obtained by Maxwell's equation describing the impedance of a heterogeneous system of dispersed low-permeable spheres (PCL) in a permeable matrix (chitosan, index  $m$ ), and given by:

$$Q = Q_m \left[ 1 + \frac{3(1 - v_m)}{\frac{q+2}{q-1} - (1 - v_m)} \right] \quad (2)$$

is plotted in Fig. 3. In this equation,  $q$  is the ratio of water vapour transmission rate of PCL to that of chitosan. The water vapour transmission rate for PCL is  $0.069 \text{ g } \mu\text{m m}^{-2} \text{ day}^{-1}$  at 100% relative humidity and is hence negligible compared to the values for chitosan and WPI. The model of Fricke [14] was derived to describe electrical conductivity in the same system as for the Maxwell equation. However, with this model the low-conducting particles can also have ellipsoidal shapes. Ellipsoidal particles, if oriented preferably parallel to the film surface, are more effective than spherical particles in decreasing the permeability. This is because the solute diffusion path is increasing with the width-to-thickness ratio of the particles. If, again, the similarity between electrical conductivity and solute permeability is drawn, it is possible to use the model here. It was considered that the PCL particles were the low-conducting ellipsoids and the chitosan polymer was the conducting or permeable matrix:

$$Q = Q_m \frac{v_m}{\tau} = Q_m \left[ \frac{\left( v_m + (1 - v_m) \frac{C_{\infty,d}}{C_{\infty,m}} \right) k_1}{1 - v_m + k_1} \right] \quad (3)$$

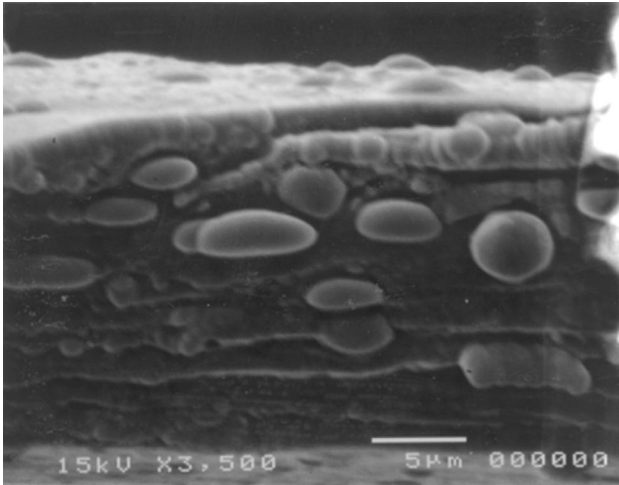


Fig. 4. SEM micrograph showing the morphology of the cross-section surface of a specimen containing 15-wt% PCL particles dispersed in the chitosan matrix.

where

$$k_1 = \frac{3k_2}{1 - k_2} \quad (4)$$

and

$$k_2 = 0.616 - \left( 0.785 - \frac{1}{\left[ \frac{w}{t} \right]} \right)^2 \quad (5)$$

where  $w$  and  $t$  are the width and thickness, respectively, of the less penetrable ellipsoids.  $C_{\infty,d}$  and  $C_{\infty,m}$  are the water saturation concentrations in the dispersed and matrix components. In this case, the ratio of water saturation concentrations in Eq. (3) vanishes. The fit yielded a width-to-thickness ratio of the dispersed PCL phase of 150. The SEM picture in Fig. 4 shows the morphology of the chitosan sample containing 18 vol% PCL (corresponding to 15 wt%). The polymers were identified by analysing the volume/area content of the different components in the micrographs. Ellipsoidal PCL particles were present, but the aspect ratio was far less than 150. The pronounced barrier improvement was hence due not only to the increase in the water diffusion path, i.e. geometrical blocking, induced by the anisotropic shape of the PCL particles and predicted by the Fricke model. The PCL particles were small (of the order of 1–10  $\mu\text{m}$ ) indicating good miscibility (compatibility) between the two components. Although the scatter in data was high, Fig. 5 indicates that the equilibrium degree of swelling and hence the water uptake decreased drastically with increasing PCL content. It seemed that PCL particles constrained the chitosan matrix phase, limiting its ability to swell freely by absorbing moisture. It is suggested that the large decrease in water vapour permeability with increasing PCL content was due both to a “geometrical blocking” of

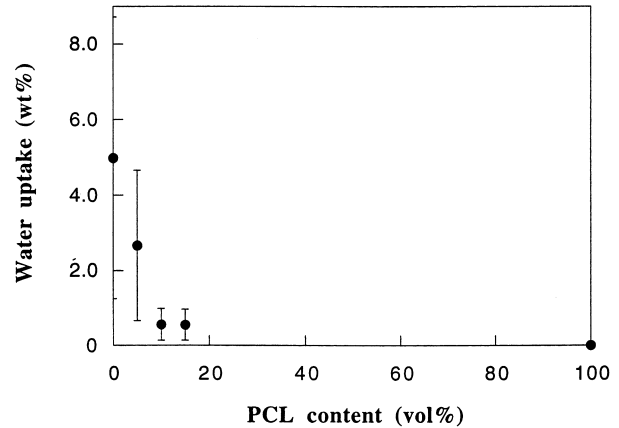


Fig. 5. Equilibrium water uptake, at a relative humidity of 11%, as a function of the PCL content in PCL/chitosan films. These values do not include strongly bound water in chitosan.

the diffusing water molecules and to a reduction in the swelling of the matrix, induced by the PCL particles.

Fig. 6 shows the water vapour transmission rate for PCL/WPI films. The water vapour barrier improvement was lower for PCL/WPI than for PCL/chitosan, although the improvement was still large. Blends with 16.8 vol% (15 wt%) PCL showed a 70% decrease in water vapour transmission rate compared with pure WPI. SEM showed that the PCL particles in this case were fibre-shaped with a cross-sectional diameter of a few micrometres (Fig. 7). The small cross-section indicated good miscibility (compatibility) between the WPI and PCL components. The Maxwell and Fricke models were applied to the system and the ratio of water saturation concentrations ( $C_{\infty,d}$  to  $C_{\infty,m}$ ) was considered negligible. The data inserted in these equations were only approximate and the results obtained served only as a guideline. The best fit of the Fricke model yielded  $w/t = 29$ , which seems high. It was believed that free swelling induced by moisture was reduced by the constraining action of the PCL particles on the matrix phase.

The densities of the PCL/chitosan and PCL/WPI systems were basically a linear function of the content of PCL, which indicated that the systems were essentially pore-free. The relatively modest temperature variations that were imposed on the blends during the solidification processes seemed to yield good adhesion between the PCL particles and the matrix phase. The PCL/chitosan blends solidified at ambient temperature and the PCL/WPI blends solidified slowly from 60°C to ambient temperature. As seen in Fig. 4, the solidification process for the chitosan system was beneficial in the sense that it provided a system with many flat PCL particles.

It was found that the water vapour transmission rates of the chitosan and the WPI films were very dependent on the way in which they were made. They were especially sensitive to the drying conditions of the solutions. It did not matter how the films were stored after the solution had evaporated and before they were conditioned in the

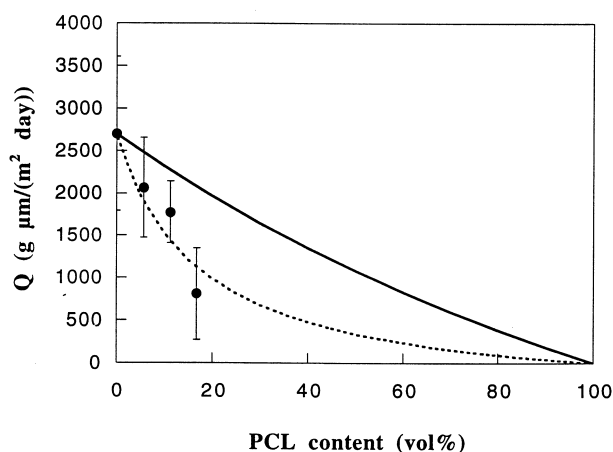


Fig. 6. Water vapour permeability ( $Q$ ) of PCL/WPI (●). The solid line is from the Maxwell equation and the broken line is the fitted curve according to the Fricke model with an aspect ratio  $w/t = 29$  for PCL.

permeability equipment. Fig. 8 shows the water vapour transmission rate of pure chitosan as a function of drying time of the solution in the vacuum oven. The drying was carried out after the chitosan solution was decanted into petri-dishes. The “zero-time” sample was dried at 30% relative humidity for 24 h. The water vapour transmission rate decreased strongly with drying time and this parameter decreased with increasing weight loss of the chitosan solution during drying. During vacuum-drying, the pH was constant at approximately 4, which indicated that both water and acetic acid evaporated. The water content of the specimens where the solution was vacuum-dried for 72 h and the films subsequently kept at 30% relative humidity

for 12 h was measured by TG, revealing a content of approximately 8 wt% water. Specimens that were dried at 30% relative humidity for 83 h contained approximately 9 wt% water. The difference in water content was very small considering the large decrease in water vapour transmission rate with increasing drying time of the solution. Fig. 9 shows the water vapour transmission rate of WPI as a function of vacuum-drying time. The drying was performed also here after the WPI solution had been decanted into petri-dishes. The “zero-time” sample was dried at 30% relative humidity for 24 h. The water vapour transmission rate decreased significantly also for WPI with increasing vacuum-drying time and correlated with the weight loss of the WPI solution. The pH decrease during vacuum-drying was very small (from 6.72 to 6.57) indicating that only water was evaporating. Thermogravimetry revealed that the water content was the same (within experimental error) for specimens where the solution was vacuum-dried for 120 h and specimens dried at 30% relative humidity (approximately 18 wt% water). These findings strongly suggest that the water content was not the only factor which was important for the barrier properties of the films. In addition, the way water was removed from the solidifying films was also important, e.g. drying time. Films that were not vacuum-dried sometimes contained visible air-bubbles. It was shown that vacuum-drying removed these bubbles. It is thus suggested that the decrease in permeability with increasing vacuum-drying time was partly due to the removal of inclusions of air from the polymer solutions.

The degree of drying and the drying procedure are also important in other respects. The gas barrier properties of these materials are very good if they are kept dry. It has

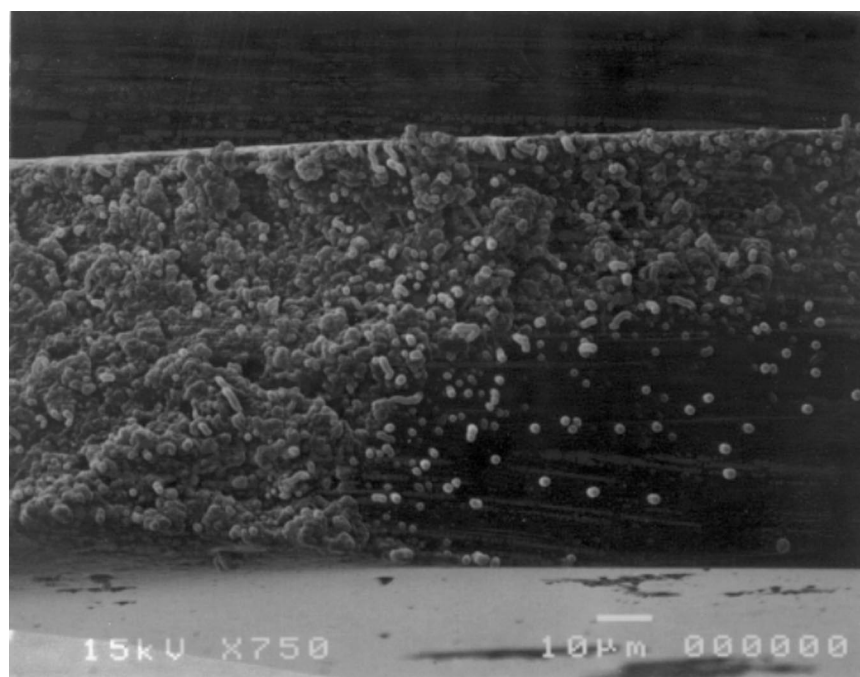


Fig. 7. SEM micrograph showing the morphology of the cross-section surface of a specimen containing 10 wt% PCL particles dispersed in the WPI matrix.

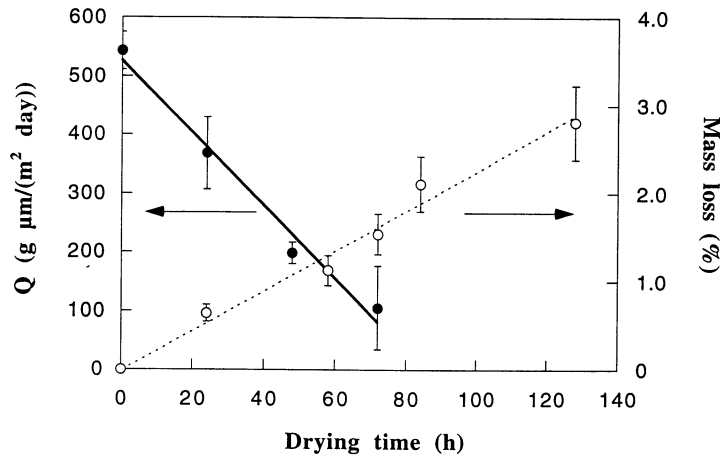


Fig. 8. Water vapour transmission rate ( $Q$ ) of films (●) and mass loss of solutions (○) of chitosan as a function of vacuum-drying time of the chitosan solution.

been shown that chitosan has an oxygen permeability which is lower than that of poly(vinylidene chloride) and similar to that of dry ethylene-co-vinyl alcohol polymers [15]. Oxygen permeabilities are given in Table 1 and the values were in reasonable agreement with earlier reported data on chitosan [15] and WPI [16].

Conventional water vapour transmission rate instruments are relatively inflexible and inefficient. There is a need to develop more flexible methods to measure water vapour transmission rates. The microcalorimeter technique was tested here in order to assess its usefulness in measuring this quantity. First, excellent agreement in water vapour transmission rates were obtained between the techniques where a LiCl solution was used on the lower side of the chitosan film and those where dehydrite was used on the lower side of the chitosan film. The technique of using dehydrite on the lower side is preferred because it allows for a rapid change in the moisture content on the upper side of the film and the water vapour transmission rates may be measured over a broad range of relative humidities in a single experiment. The water vapour transmission rate increased slightly with increasing water vapour activity

above  $a_1 = 0.15$  (Fig. 10). The observed minimum at  $a_1 = 0.1-0.15$  might be due to antiplasticisation effects. However, in order to draw this conclusion, further measurements are needed. The water vapour transmission rates obtained with the Mocon-instrument were slightly higher than the values obtained by the microcalorimeter. Values obtained by Butler et al. [15] on glycerin-plasticised chitosan are also presented in Fig. 10. These values were slightly higher than the values determined here by the

Table 1  
Oxygen permeability at 25°C and 0% RH

Material	$P^a$ (cm <sup>3</sup> (STP) μm m <sup>-2</sup> day <sup>-1</sup> atm <sup>-1</sup> )
Chitosan	33 ± 15
PCL/chitosan (5 wt%/95 wt%)	11 ± 6
PCL/chitosan (10/90)	5 ± 5
PCL/chitosan (15/85)	28 ± 12
PCL	17 200 ± 300
WPI	29 ± 16

<sup>a</sup> Averages of at least two measurements.

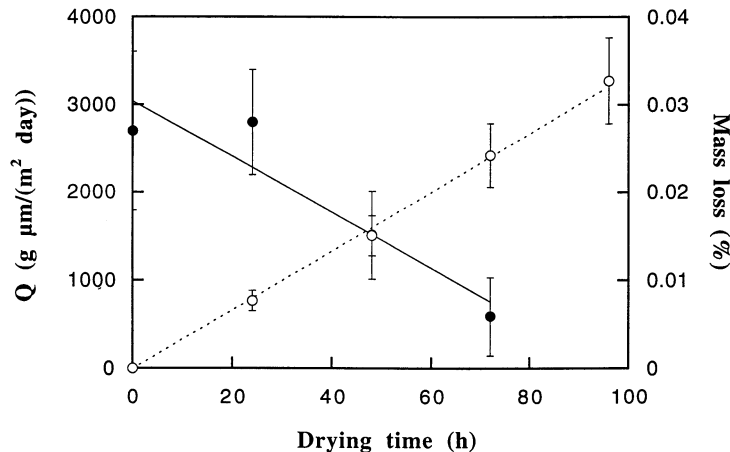


Fig. 9. Water vapour transmission rate ( $Q$ ) of films (●) and mass loss of solutions (○) of WPI as a function of vacuum-drying time of the chitosan solution.

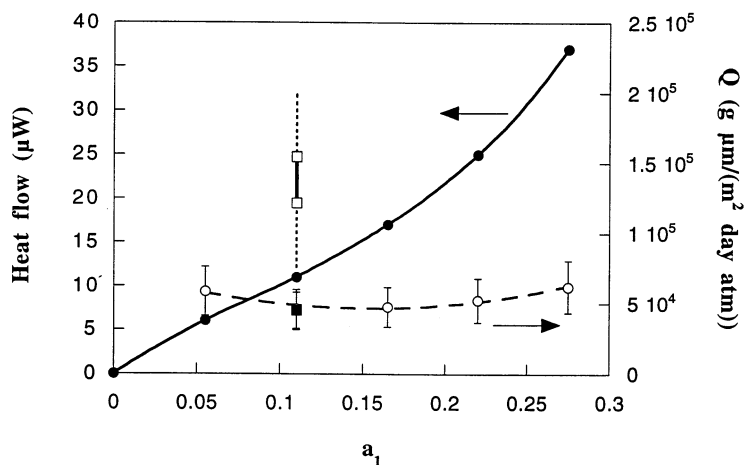


Fig. 10. Heat flow rate generated due to sorption of water in dehydrite which is placed in the lower side of the chitosan film (●) and corresponding water vapour transmission rates ( $Q$ ) through the chitosan film (○). The water vapour transmission rate ( $Q$ ) through the chitosan film with LiCl solution on the lower side of the film and dry nitrogen gas flowing on the upper side of the film is given by (■). Also shown are the water vapour transmission rates determined by the Mocon instrument (□) and literature data [15] on glycerin-plasticised chitosan (broken line).

microcalorimeter. This was indeed expected, since the specimens were unplasticised. Hence, it seemed that the water vapour transmission rates determined by the Mocon instrument were slightly too high. Reported relative errors of standard permeability (Mocon)-tests range between 6 and 20% [17]. The relative error in the measured microcalorimeter permeabilities given here is estimated to be 30% based on repeated values and the many parameters involved in the calculations. This relative error may seem large but it is many times acceptable.

#### 4. Conclusions

Blends with a volume fraction of 18.3% PCL particles lowered the water vapour transmission rate of chitosan by 90%. 16.8 vol% PCL particles lowered the water vapour transmission rate of WPI by 70%. These large reductions were due partly to the fact that a major portion of the PCL particles were either ellipsoidal (in chitosan) or fibrous (in WPI). The large reductions were also due to a constraining action of the PCL particles, effectively reducing the swelling of the matrix phase. Density and SEM revealed good adhesion between PCL and the matrices. The water vapour transmission rate of the films decreased with increasing solution drying time. This was suggested to be due partly to the removal of air-bubbles from the solution. A new very flexible technique for measuring water vapour transmission rate was developed, based on microcalorimetry.

#### Acknowledgements

This work was sponsored by a grant from Bizkaiko Foru Aldundia, Spain. M. Lundbäck, Department of Polymer Technology, Royal Institute of Technology, A. Hellman and L. Höjvall at Packforsk are thanked for experimental assistance.

#### References

- [1] Chen HJ. Dairy Sci 1995;78:2563.
- [2] Knorr D. Food Technol 1991;January:114.
- [3] Guilbert S, Cuq B, Gontard N. Food Addit Contam 1997;14:741.
- [4] Kittur FS, Kumar KR, Tharanathan RN. Z Lebensm Forsch 1998;206:44.
- [5] Shellhammer TH, Krochta JM. J Food Sci 1997;62:390.
- [6] Anker M, Stading M, Hermansson A-M. J Agric Food Chem 1998;46:1820.
- [7] McHugh TH, Krochta JM. J Agric Food Chem 1994;42:841.
- [8] Kinsella JE, Whitehead DW. Adv Food Nutrit 1989;33:343.
- [9] Kinsella JE. CRC Crit Rev Food Sci 1984;21:197.
- [10] Greener Donhowe IK, Fennema OR. In: Krotcha JM, Baldwin EA, Nisperos-Carriedo M, editors. Edible coatings and films to improve food quality. Lancaster, PA: Technomic Publishing Company Inc, 1994.
- [11] Krook M, Hedenqvist MS, Albertsson A-C, Hellman A, Iversen T, Gedde UW. Polym Engng Sci 2000;40:143.
- [12] Suurkuusk J, Wadsö I. Chem Ser 1982;20:155.
- [13] Hedenqvist M, Gedde UW. Prog Polym Sci 1996;21:299.
- [14] Fricke H. Phys Rev 1924;24:575.
- [15] Butler BL, Vergano PJ, Testin RF, Bunn JM, Wiles JL. J Food Sci 1996;61:953.
- [16] McHugh TH, Krochta JM. J Am Oil Chem Soc 1994;71:307.
- [17] Hedenqvist M, Gedde UW. Packag Techn Sci 1999;12:131.